

Evaluation of a Façade Integrated Concentrating Solar Collector System

Piratheepan Mahendran¹, and Timothy Anderson¹

¹Auckland University of Technology, Auckland, New Zealand

Abstract

The use of building integrated photovoltaic/thermal (BIPVT) collector modules is one of the most effective ways to harness the solar energy within the building environment. Using static reflectors along with BIPVT absorbers may be a cost effective way to utilize these in façade applications. In order to precisely predict the overall performance of such building integrated façade collectors it is crucial to develop a mathematical model that represents such systems. As such, a mathematical model was developed to describe the performance of a façade integrated BIPVT solar concentrator system and subsequently this was validated with a physical prototype.

Using the validated model, a sensitivity analysis was performed to determine the design parameters that significantly influence the efficiency of the collector. It was shown that key parameters such as tube spacing and thermal conductivity between the solar cell and the absorber have a significant effect on the overall efficiency while mass flow rate does not have any significant effect on the overall performance.

Keywords: *building integrated photovoltaic/thermal, façade, concentrator, BIPVT*

1. Introduction

Energy consumption in the built environment accounts for nearly one third of the global energy demand (IEA 2011). A significant portion of this could be met through onsite energy generation utilising solar energy, while intelligent building design practices and incorporating solar energy systems within the building envelope are two solutions that could reduce the long term energy costs and reduce environmental impacts. However, traditional solar energy systems such as photovoltaic panels or solar thermal collectors retrofitted onto buildings after they have been built may result in poor aesthetics and sub-optimal energy outputs. Therefore, integration of combined photovoltaic/solar thermal collectors into a buildings fabric could give greater opportunity for the use of renewable energy technologies in buildings.

Generating thermal and electrical energy simultaneously from solar irradiation using photovoltaic/thermal (PV/T) systems is an area of research that has received significant attention in recent years (Ibrahim et al. 2014, Fudholi et al. 2014, Tripanagnostopoulos 2012). However, there have been relatively few attempts to utilize such systems with low concentration ratio concentrating systems to increase the radiation incident on the PV/T absorber, and even fewer that incorporate such systems into the fabric of a building. A significant advantage of low concentration reflectors is that they do not need to track the sun making them ideal for integration into a building's façade, though by doing this they will have a lower acceptance angle range compared with tracking collectors (Rabl 1976). Despite this disadvantage, low concentration ratio collectors offer the advantage of collecting diffuse radiation as well as the beam component (Petter et al. 2012). This increases the possibility of using the traditional Si solar cells with less need for precise optics.

In 2002 Tripanagnostopoulos et al (2002) analysed PV/T combined collectors incorporating low concentration ratio booster reflectors with a view to achieving high combined efficiency. In a parallel study, (Tselepis and Tripanagnostopoulos 2002) performed a life cycle assessment of the combined collector and concluded that they were more cost competitive, had a shorter payback time and less environmental impact than that of standalone PV panels. As such, the combination of low concentration ratio reflective elements along with hybrid absorbers may further improve the cost competitiveness of the system by increasing the radiation on the absorber plate.

Despite the work showing the benefits of using reflectors with PV/T absorbers, there are few studies that have investigated systems with a static reflector combined with a hybrid absorber plate for façade applications. A study by Gajbert, et al. (2007) found that low concentration ratio PV/T modules have advantages over traditional modules and proposed a PV/T collector with a parabolic reflector. However there appears to be few active attempts to utilise concentrating BIPVT systems, and a lack of detail in describing their combined thermal/electrical performances.

In light of this, this study examines the performance of a façade integrated solar collector that incorporates a flat reflective element with a view to increasing the radiation on a photovoltaic/thermal (PV/T) absorber plate, as shown in Figure 1.

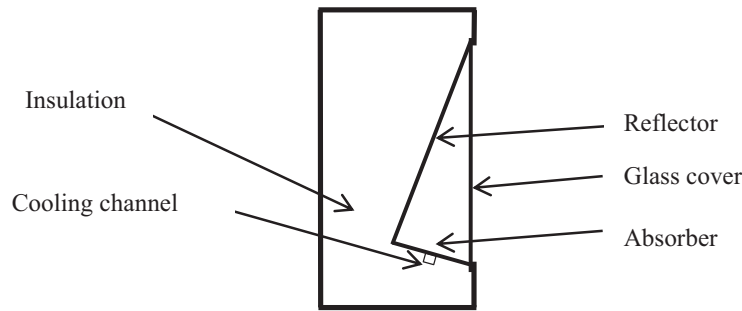


Fig. 1: Façade Integrated Concentrator

2. Mathematical model

In order to analyse the performance of the proposed façade integrated collector, a one dimensional steady state thermal model was developed. A simplified thermal resistance network as shown in Figure 2 was used to undertake a heat balance of the absorber plate.

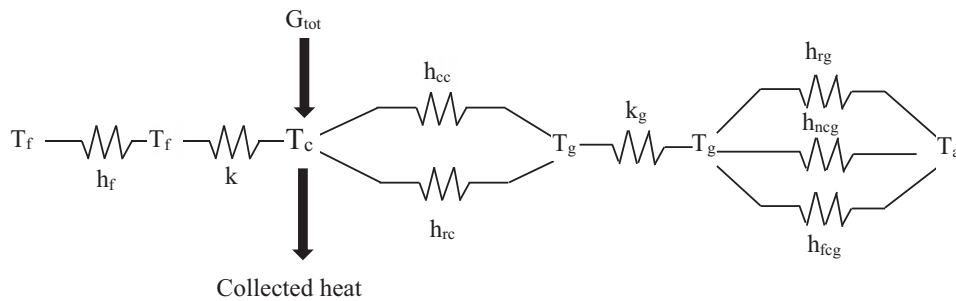


Fig. 2: Simple thermal network of the proposed module

For a typical solar thermal collector, the useful thermal energy gain Q can be determined from equation 1.

$$Q = AF_R[(\tau\alpha)_{PV}G - U_L(T_i - T_a)] \quad (\text{eq. 1})$$

This equation can be further modified, as shown in equation 2, to incorporate the concentration ratio C of the proposed low concentration collector.

$$Q = AF_R[(\tau\alpha)_{PV}G.C - U_L(T_i - T_a)] \quad (\text{eq. 2})$$

Here Q is given by a function of absorber area (A), heat removal factor (F_r), the transmittance-absorptance product for the photovoltaic absorber ($(\tau\alpha)_{PV}$), the solar radiation (G), the concentration ratio (C), the overall heat loss coefficient (U_L) and the temperature difference between inlet and the ambient temperature.

In practice it is not possible to cover the whole absorber module with photovoltaic cells, hence equation 2 can be further modified to include a packing factor (S) and the transmittance-absorptance product of the thermal absorber and the PV material, as shown in equation 3.

$$Q = S[AF_R[(\tau\alpha)_{PV}G.C - U_L(T_i - T_a)]] + (1 - S)[AF_R[(\tau\alpha)_T G.C - U_L(T_i - T_a)]] \quad (\text{eq. 3})$$

The ratio of the heat collected against the irradiation falling on the absorber plate gives the thermal efficiency of the collector as shown in equation 4

$$\eta_{thermal} = F_R[S(\tau\alpha)_{PV} + (1 - S)(\tau\alpha)_T] - F_R U_L \frac{(T_i - T_a)}{GC} \quad (\text{eq. 4})$$

Following on from this, to determine the optical concentration ratio in terms of the radiation reaching the absorber, equation 5 can be used (Kostic L et al. 2010).

$$C = \frac{G_{tot}}{G_{net}} \quad (\text{eq. 5})$$

Where G_{tot} is the sum of the radiation directly falling on the absorber G_{dir} and the radiation from the reflector G_{ref} on the absorber, while G_{net} is the amount of radiation received by a horizontal absorber alone without the reflector. By incorporating the reflectance ρ_{Al} of the reflector, C can be expressed as equation 6

$$C = \frac{G_{dir} + \rho_{Al} G_{ref}}{G_{tot}} \quad (\text{eq. 6})$$

Now from the work of Piratheepan and Anderson (2014), and basic geometry, the relationship for the average optical concentration ratio C for the proposed collector can then be expressed by equation 7. Where α is the elevation angle of the sun and the γ is the inclination angle of absorber relative to the horizontal.

$$C = \begin{cases} \left[\frac{\cos(\alpha+\gamma)(\tan(\alpha+\gamma)+\tan\gamma)}{\sin\alpha} \right] \rho_{Al} + \frac{1}{\cos\gamma} & \alpha < (90 - 2\gamma) \\ \left[\frac{\cos(\alpha+\gamma)(3+\tan\gamma)}{\sin\alpha} \right] \rho_{Al} + \frac{1}{\cos\gamma} & (90 - 2\gamma) < \alpha < (90 - \gamma) \\ \frac{\sin(\alpha+\gamma)(1-3\tan(\alpha+\gamma-90))(\tan(\alpha-(90-\gamma)))}{\sin\alpha} & (90 - \gamma) < \alpha < 90 \end{cases} \quad (\text{eq. 7})$$

Furthermore, the collector heat removal efficiency factor (F_r) can be expressed in terms of heat loss coefficient (U_L), mass flow rate (m) and the collector efficiency factor (F') as given by equation 8.

$$F_r = \frac{mC_p}{A} \left[1 - \exp\left(-\frac{AU_L F'}{mC_p}\right) \right] \quad (\text{eq. 8})$$

The collector efficiency factor (F') can be calculated using equation 9 in terms of its fin efficiency factor F .

$$F' = \frac{1/U_L}{\left[\frac{1}{U_L[d+(w-d)F]} + \frac{1}{wh_{PV}A} + \frac{1}{\pi dh_{fl}} \right]} \quad (\text{eq. 9})$$

Here $h_{PV/A}$ accounts for the bond resistance between the PV cell and the absorber plate as shown by (Zondag et al. 2002). The forced convection heat transfer coefficient (h_{fl}) in the cooling tube can be determined from equation 10.

$$h_{fl} = \frac{Nu \cdot k_f}{d} \quad (\text{eq. 10})$$

Where k_f is the conductivity of the fluid at the mean temperature and Nu is the Nusselt number that can be determined from any number of relationships for forced convective heat transfer in a tube, in this study the Gnielinski (Cengel 2007) correlation was used.

In order to calculate the fin efficiency factor F , it is necessary to calculate the coefficient (M) that accounts for the overall thermal conductivity and the thickness of the PV/T absorber plate as given by equation 11 in terms of overall thermal loss coefficient U_L .

$$M = \sqrt{\frac{U_L}{k_{abs}L_{abs} + K_{PV}L_{PV}}} \quad (\text{eq. 11})$$

As such, the modified fin efficiency F can be calculated using equation 12, where w is the tube spacing and d is the hydraulic diameter of the tube.

$$F = \frac{\tanh\left[\frac{M(w-d)}{2}\right]}{\frac{M(w-d)}{2}} \quad (\text{eq. 12})$$

In the determination of M in equation 9, the overall thermal loss coefficient U_L is the sum of the heat losses via top, rear and edge of the collector as given by equation 13.

$$U_L = U_{top} + U_{rear} + U_{edge} \quad (\text{eq. 13})$$

As the rear heat loss and edge losses are mainly through the insulation, the rear loss coefficient U_{rear} and the edge loss coefficient U_{edge} can be determined from Fourier's Law.

However, in the determination of the top losses the glazing on the proposed collector, as shown in Figure 1, is not parallel to the absorber plate. Recently though (Piratheepan et al. 2014) showed that the natural convection heat loss in an air filled enclosure such as this could be predicted by equation 14, where b is the breadth of the absorber and h is the height of the reflector.

$$Nu = 0.67Ra^{0.36}\left(\frac{b}{h}\right)^{1.75} \quad (\text{eq. 14})$$

This can subsequently be rearranged to determine the value of the natural convection heat transfer coefficient h_{cc} inside the concentrator enclosure

To estimate the radiation heat transfer coefficient inside the concentrator h_{rc} the enclosure was assumed to be a two-surface enclosure consisting of the absorber plate and the glazing by assuming the reflector is adiabatic. Hence the expression of the h_{rc} can be written in terms of area of the absorber plate (A), area of the glazing (A_g), the view factor (F_{cg}) from the absorber to the glazing, and the emittance of absorber plate and the glazing ε_p and ε_g , as expressed in Equation 15.

$$h_{rc} = \frac{\sigma(T_{pm}^4 - T_g^4)}{\left(\frac{1-\varepsilon_c}{A\varepsilon_c}\right) + \left(\frac{1}{AF_{cg}}\right) + \left(\frac{1-\varepsilon_g}{A_g\varepsilon_g}\right)} \quad (\text{eq. 15})$$

Where T_{pm} and T_g are the mean plate temperature and the internal glazing temperature of the collector respectively.

The view factor F_{cg} can be deduced from equation 16 in terms of enclosure dimensions

$$F_{cg} = \frac{2b}{b\left(1 + \frac{1}{\sin\beta}\right) - h} \quad (\text{eq. 16})$$

Subsequently, the heat loss through the glass cover can be calculated using the heat transfer coefficient of the glass k_g internal glazing temperature T_g and external glazing temperature T_g' .

Now, the external heat loss from the glazed cover is the sum of the radiation, natural and the forced convection heat losses. As majority of the collector faces the ambient environment, it was assumed that the glass cover radiated heat to the surroundings with an ambient temperature T_a . Hence, the radiation heat transfer coefficient from the glazing h_{rcg} can be expressed in terms of external glazing temperature T_g' and the ambient temperature T_a as shown in equation 17

$$h_{rcg} = \sigma\varepsilon_g(T_g'^2 + T_a^2)(T_g' + T_a) \quad (\text{eq. 17})$$

Furthermore, the losses due to natural and forced convection also must be taken in to account. The forced convection heat transfer coefficient h_{fcg} will be a function of velocity of the wind, an approximation of which can be expressed by equation 18, where v is the wind velocity.

$$h_{fcg} = 4.214 + 3.575V \quad (\text{eq. 18})$$

The natural heat transfer coefficient h_{ncg} can be expressed by equation 19

$$h_{ncg} = 1.78(T_g' - T_a)^{1/3} \quad (\text{eq. 19})$$

Using this approximation it is possible to calculate the overall convection heat transfer coefficient h_c by

integrating both forced and natural heat transfer coefficient using equation 20 (Eicker 2006)

$$h_c = (h_{fcg}^3 + h_{ncg}^3)^{1/3} \quad (\text{eq. 20})$$

In summary; the combination of heat losses and the total useful energy extracted, considering the energy balance of the collector, mean the thermal efficiency of the façade integrated collector can be established.

Now in examining the electrical performance of the system, one trade-off of using silicon solar cells under concentrated radiation is that their efficiency degrades with the temperature increase. Hence it is essential to express the electrical efficiency in terms of the temperature of the absorber plate.

The electrical efficiency of the solar cell can be determined by firstly determining the power generated by the cell at its maximum power point, as given by equation 21.

$$P = I_{mp} V_{mp} \quad (\text{eq. 21})$$

This can also be expressed in terms of fill factor (FF) and the open circuit voltage V_{oc} and short circuit current I_{sc} as shown in equation 22.

$$P = FF I_{sc} V_{oc} \quad (\text{eq. 22})$$

However, V_{oc} and FF decrease significantly with increased temperature, while short circuit current increases marginally with the temperature (Zondag 2008). Taking this into account using equation 23 (Dubey et al. 2013) gives a good approximation of the electrical efficiency of a photovoltaic cells under various temperatures given that the nominal operating cell temperature ($NOCT$) and the temperature coefficient (β) and the efficiency of the cell at $NOCT$ conditions are known from the manufacturer's datasheet.

$$\eta_e = \eta_{NOCT} (1 - \beta(T_{pm} - NOCT)) \quad (\text{eq. 23})$$

for typical crystalline Si modules β can be assumed as 0.004 (Notton et al. 2005).

When the packing factor S is taken in to account, the electrical efficiency of the collector on a relative area basis η_{elect} can be expressed by equation 24.

$$\eta_{elect} = \eta_{NOCT} (1 - \beta(T_{pm} - NOCT)) * S \quad (\text{eq. 24})$$

By combining equation 4 and equation 2 the combined efficiency η_{tot} of the collector can be calculated from equation 25.

$$\eta_{tot} = \eta_{thermal} + \eta_{elect} \quad (\text{eq. 25})$$

3. Experimental testing and results

In order to validate the mathematical model and findings derived from its use, it is necessary to compare the outcome with an experimental model. As there is no standard method for testing photovoltaic/thermal hybrid modules it was decided use a standard steady state test method similar to the one describing the thermal performance of glazed liquid heating collectors given in AS/NZS 2535.1 (2007). As such, an experimental testing system was constructed on the roof of Auckland University of Technology's School of Engineering building, facing true north. In doing this, T-type thermocouples were used to measure the inlet and the outlet of the coolant as well as the ambient temperature. A cup anemometer and a wind vane were mounted adjacent to the collector to measure the wind speed and direction. Finally, a Delta-T SPN1 type sunshine pyranometer was used to measure the beam and diffuse radiation. For the electrical output, the voltage and current were measured simultaneously while keeping the system loaded at maximum power point.

Now, fabrication of the façade collector involves three main parts; the PV/T absorber, the reflector and the insulation elements including the glass cover. For this work the finned tube absorber plate was fabricated from a 1.2 m length of 2 mm aluminium painted matte black, with two absorbers mounted in series. A 10 mm square aluminium tube was attached to the back of each absorber using a thermally conductive adhesive to act as the

cooling channel. Square tube was used as it provides a larger contact surface between the absorber plate and the cooling tube, thus improving the fin efficiency. Each absorber plate was then fitted with a custom made string of seven 150 mm crystalline solar cells connected in series and bonded to the absorber using a silicone conformal coating. This thin layer of clear conformal coating protects the cells under extreme environmental and climatic condition and insulates the rear wiring of the solar cells when the absorber is exposed to the concentrated radiation. Reflector was prepared by attaching a silver metalized film on an aluminum sheet.

Due to the practical issues associated with integrating the façade integrated collector into an actual building façade, two vertical “wall” sections were fabricated to mount the concentrators. Each wall was packed with mineral wool insulation (R2.8) to insulate the rear of the concentrator, and replicate a building façade, while the front surface was glazed using a low-iron glass cover. A schematic representation of the combined collector test system is shown in figure 3.

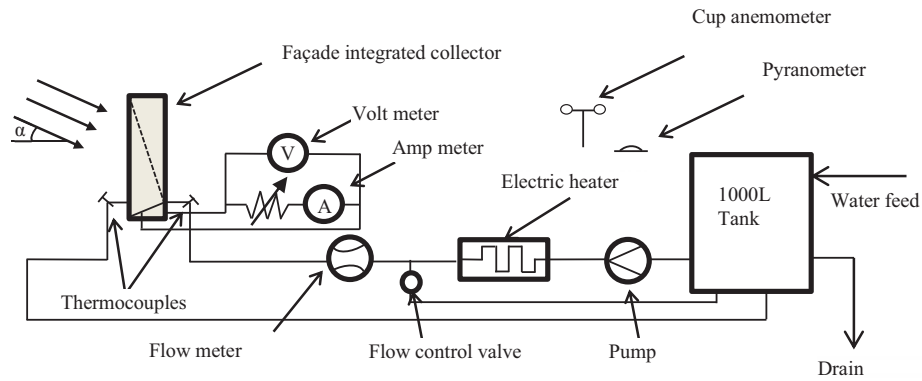


Fig. 3: Experimental test rig and the circuit diagram for electrical measurements

In summary, the design parameters of the prototype collector tested here are given in table 1.

Table. 1: Physical characteristics of experimental prototype

Parameter	Symbol	Value	Unit
System flow rate	m	1.33×10^{-5}	m^3/S
Collector length	L	2.4	m
Collector breath	b	0.2	m
Reflector height	h	0.6	m
Collector area	A	0.48	m^2
PV Transmit/absorpt	$\tau\alpha_{PV}$	0.78 (De Vries 1998)	-
Thermal Transm/absorpt	$\tau\alpha_T$	0.925 (Anderson et al. 2009)	-
Absorber thickness	L_{abs}	0.002	m
PV thickness	L_{PV}	0.0004	m
PV conductivity	K_{PV}	130	W/mK
Tube hydraulic diameter	d	0.0088	m
Tube spacing	w	0.2	m
Cell-absorber Quasi heat transfer coefficient	h_{PVA}	45	$\text{W}/\text{m}^2\text{K}$
Insulation conductance	k_{ins}	0.045	W/mK
Back insulation thickness	L_{ins}	0.1	m

Edge insulation thickness	L_{edge}	0.025	m
Absorber conductivity	K_{abs}	130	W/mK
Packing factor	S	0.7	-
Conductance of glass	k_g	0.9	W/mK
Reflectance of silver metalized film	ρ_{Al}	0.9	-

3.1 Experimental results and model validation

To validate the mathematical model several sets of readings were taken from the test rig under various solar elevation angles and input temperatures. These were taken when the sun was near solar noon, such that the effect of shading, due to the design of mounting enclosure, was minimised. As shown in figure 4 the mathematical model incorporating with new heat transfer relationships for the concentrator, as well as the concentration ratio, is capable of predicting the performance with good accuracy.

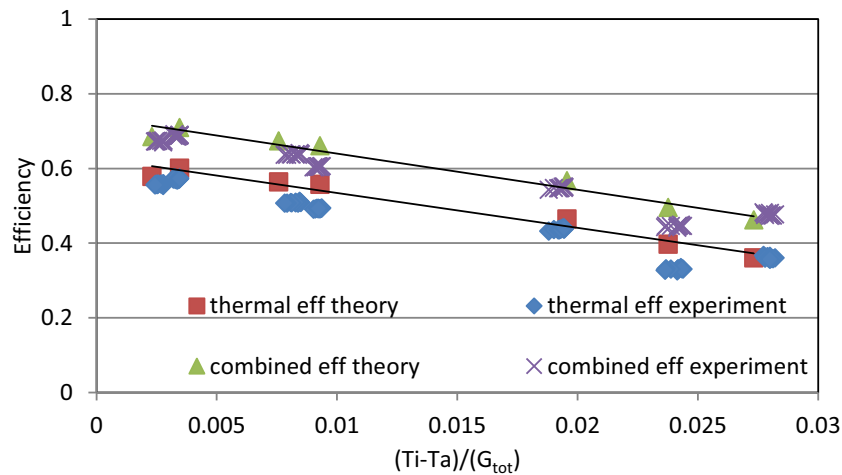


Fig. 4: Experimental and theoretical efficiencies of façade integrated collector

3.2 Modelling Results

Now in table 1, there are number parameters which can be modified to improve the performance of the collector. Hence, having validated the mathematical model it was used to perform a sensitivity analysis on the system. In this study, only one design variable was varied at a time and the effect of that particular parameter on the efficiency was observed. This allows us to determine the design variables that are critical in terms of efficiency of the system and its design.

In the concentrator it is likely that high temperatures will be achieved and so there is a need for improved cooling. Heat transfer in the cooling channel is a function of Reynold's number and thus varying the flow rate may have the effect on the overall efficiency of the collector. However as shown on figure 5, the efficiency of the collector does not significantly improve with the increased fluid flow rate. The slight increase in efficiency can be attributed to an increase in the turbulence in the system increasing the heat transfer marginally. Furthermore, a reduction in temperature will increase the electrical efficiency marginally though the pumping power required to achieve this may offset any gains by doing this.

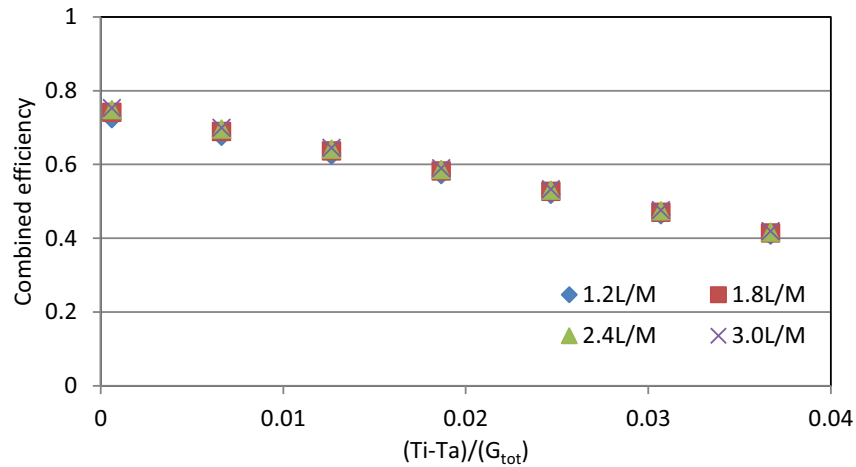


Fig. 5: Combined efficiency by varying flow rate

Another means of improving the efficiency could be to reduce the width of the absorber for a single tube, or by decreasing the spacing between adjacent tubes in systems with multiple cooling tubes. As shown in figure 6, this will increase the efficiency significantly. This can be explained by the fact that an increase in the number of tubes across the absorber plate improves the fin efficiency and thus increases the performance of the collector. However it can be seen that, at higher $(Ti-Ta)/G \cdot C$ values they tend to converge. This suggest that although decreasing the tube spacing increases the efficiency initially, there are other factors which will decrease the efficiency at higher $(Ti-Ta)/G \cdot C$.

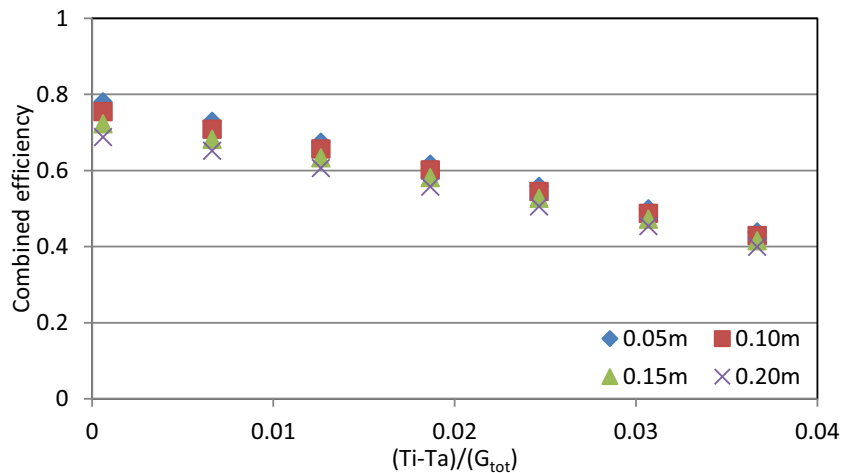


Fig. 6: Combined efficiency by varying tube spacing

Further, the combined efficiency of the collector could be also improved by improving the heat transfer coefficient between the solar cells and the thermal absorber. Unlike a thermal collector that has a bond resistance between the tube and absorber (Duffie and Beckman 2006), a “quasi” heat transfer coefficient, with a value of $45\text{W/m}^2\text{K}$, between the PV cells and the absorber plate is used (Zondag et al. 2002). Based on this Anderson et al (2009) stated that this thermal conductance might be improved by means introducing a thermally conductive adhesive. Following on from this recommendation, it can be seen in figure 7, that when the heat transfer coefficient is doubled from $30\text{W/m}^2\text{K}$ to $60\text{W/m}^2\text{K}$ the efficiency is improved by approximately 10%.

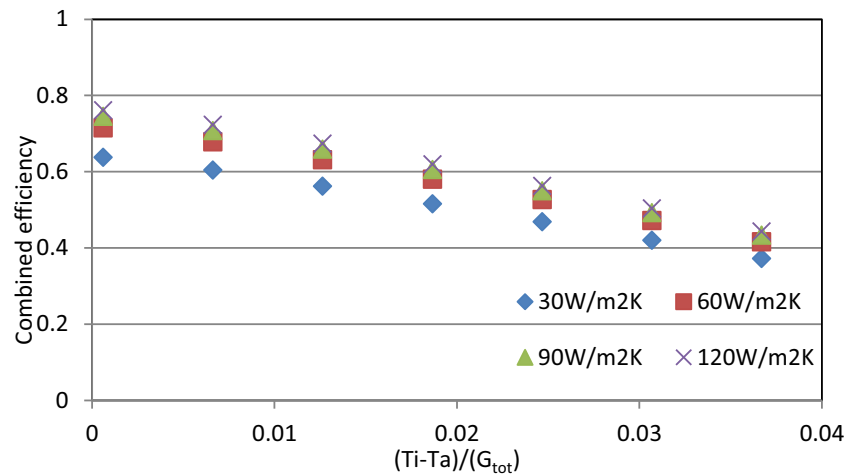


Fig. 7: Combined efficiency by varying cell to absorber heat transfer coefficient

4. Conclusion

From the results, it was shown that the mathematical model incorporated with the heat transfer empirical relationships presented in this paper was able to predict the performance of the particular system. Further, from the sensitivity analysis, there are number of conclusions that can be drawn. Firstly, increasing the flowrate in the cooling tubes appears to offer little benefit with respect to increasing the efficiency of the collector.

However, the combined efficiency of the collector can be improved by increasing the number of cooling channels across the absorber plate though this may not be economical. Hence increasing the number tubes has to be considered as a trade-off between the efficiency and the cost of the collector. Finally, improved thermal contact between the solar cells and the thermal absorber will increase the efficiency dramatically and appears to offer significant potential in improving the performance of the façade integrated BIPVT solar concentrator system.

5. References

- Anderson, T. N., Duke, M., Morrison, G.L and Carson, J. K. 2009 Performance of a building integrated photovoltaic/thermal (BIPVT) solar collector. *Solar Energy*, Vol 83, pp. 445-455.
- AS/NZS 2535.1, 2007. Test methods for solar collectors. Part 1: thermal performance of glazed liquid heating collectors including pressure drop. Standards Australia, Homebush.
- Cengel, Y. A. 2007. Heat and mass transfer: a practical approach, 3rd ed., McGraw-Hill, Boston.
- De Vries, D.W., 1998. Design of a photovoltaic/Thermal Combi-panel, PhD Thesis. Eindhoven University.
- Dubey, S., Sarvaiya, J. N and Seshadri B. 2013 Temperature Dependent Photovoltaic (PV) Efficiency and Its Effect on PV Production in the World – A Review. *Energy Procedia*, Vol 33, pp. 311-321.
- Duffie, J. A and Beckman W. A. 2006. *Solar Engineering of Thermal Processes*. In *Solar Engineering of Thermal Processes*, Wiley, New York.
- Eicker, U. 2006. *Solar technologies for buildings*. John Wiley & Sons, Chichester.
- Gajbert, H., Hall, M and Karlsson, B., 2007, Optimisation of reflector and module geometries for stationary, low-concentrating, facade-integrated photovoltaic systems, *Solar Energy Materials and Solar Cells*, Vol. 91, pp. 1788-1799.
- Fudholi, A., Sopian, K. Yazdi., M. H. Ruslan., M. H. Ibrahim A and Kazem H. A. 2014. Performance analysis of photovoltaic thermal (PVT) water collectors. *Energy Conversion and Management*, Vol 78, pp 641-651.

Ibrahim, A., Fudholi, A., Sopian, K., Othman M. Y and Ruslan M. H. (2014) Efficiencies and improvement potential of building integrated photovoltaic thermal (BIPVT) system. *Energy Conversion and Management*, Vol 77, pp 527-534.

IEA, International energy agency 2011. *Solar energy perspectives: OECD/IEA*, France.

Kostic, L.T., Pavlovic, T.M and Pavlovic Z.T (2010) Optimal design of orientation of PV/T collector with reflectors. *Applied Energy*, Vol 87, pp 3023-3029.

Krauter, S.C.W 2006. *Solar electric power generation*. Heidelberg: Springer-Verlag.

Notton, G., Cristofari, C., Mattei, M and Poggi P 2005, Modelling of a double-glass photovoltaic module using finite differences. *Applied Thermal Engineering*, Vol 25, pp 2854-2877.

Petter, B., Breivik, C., and Drolsum R 2012, Building integrated photovoltaic products: A state-of-the-art review and future research opportunities. *Solar Energy Materials and Solar Cells*, Vol 100, pp 69-96.

Piratheepan, M. and Anderson, T. N 2014, Experimental evaluation of low concentration collectors for façade applications. *Proceedings of the 52nd Annual Australian Solar Council Scientific Conference*, Melbourne, May 2014.

Piratheepan, M., Anderson T. N and Saiful S., 2014, Experimental Evaluation of Natural Heat Transfer in Façade Integrated Triangular Enclosures. *Proceedings of the 1st Annual Asia-Pacific Solar Research Conference*, Sydney, October 2014

Rabl, A. 1976. Comparison of solar concentrators. *Solar Energy*, Vol 18, pp 93-111.

Tripanagnostopoulos, Y. 2012, Photovoltaic/thermal solar collectors. In *Comprehensive Renewable Energy*, Vol 3, pp 255-300. Elsevier Oxford.

Tripanagnostopoulos, Y., Nousia, T., Souliotis, M and Yianoulis, P. 2002, Hybrid photovoltaic/thermal solar systems. *Solar Energy*, Vol 72, pp 217-234.

Tselepis, S. & Tripanagnostopoulos Y. 2002, Economic analysis of hybrid photovoltaic/thermal solar systems and comparison with standard PV modules. In *Proceedings of the international conference PV in Europe*, Rome, October 2012.

Zondag, H. A., 2008 Flat-plate PV-Thermal collectors and systems: A review. *Renewable and Sustainable Energy Reviews*, Vol 12, pp 891-959.

Zondag, H., De Vries, D., Van Helden, W., Van Zolingen R and Van Steenhoven A., (2002) The thermal and electrical yield of a PV-thermal collector. *Solar Energy*, Vol 72, pp 113-128.